J|A|C|S ARTICLES

Published on Web 04/12/2010

Similar Topological Origin of Chiral Centers in Organic and Nanoscale Inorganic Structures: Effect of Stabilizer Chirality on Optical Isomerism and Growth of CdTe Nanocrystals

Yunlong Zhou,[†] Ming Yang,[‡] Kai Sun,[§] Zhiyong Tang,*[,†] and Nicholas A. Kotov*[,‡,§]

National Centre for Nanoscience and Technology, Beijing 100190, People's Republic of China, and Department of Chemical Engineering and Department of Materials Science and Engineering, University of Michigan, Ann Arbor, Michigan 48109

Received August 19, 2009; E-mail: zytang@nanoctr.cn; kotov@umich.edu

Abstract: It is observed in this study that the chirality of cysteine stabilizers has a distinct effect on both the growth kinetics and the optical properties of CdTe nanocrystals synthesized in aqueous solution. The effect was studied by circular dichroism spectroscopy, temporal UV−vis spectroscopy, photoluminescence spectroscopy, and several other microscopy and spectroscopic techniques including atomic modeling. Detailed analysis of the entirety of experimental and theoretical data led to the hypothesis that the atomic origin of chiral sites in nanocrystals is topologically similar to that in organic compounds. Since atoms in CdTe nanocrystals are arranged as tetrahedrons, chirality can occur when all four atomic positions have chemical differences. This can happen in apexes of nanocrystals, which are the most susceptible to chemical modification and substitution. Quantum mechanical calculations reveal that the thermodynamically preferred configuration of CdTe nanocrystals is *S* type when the stabilizer is D-cysteine and *R* type when L-cysteine is used as a stabilizer, which correlates well with the experimental kinetics of particle growth. These findings help clarify the nature of chirality in inorganic nanomaterials, the methods of selective production of optical isomers of nanocrystals, the influence of chiral biomolecules on the nanoscale crystallization, and practical perspectives of chiral nanomaterials for optics and medicine.

Introduction

Colloidal semiconductor nanocrystals (NCs) with unique optical properties are receiving intensive attention in the fields of both fundamental science and technological application.[1−3] Most of the research in NC optics had been carried out regarding emission or adsorption properties of NCs.[4,5] Much less attention was given to chiral properties of colloidal semiconductor NCs,[6,7] while the importance of such properties for both optical and biological materials made on the basis of NCs can be truly tremendous. Combined with large quantum confinement and catalytic properties of NCs, chiral effects can give rise to new incarnations of traditional optical devices, such as flexible displays and highly selective enantiometric reactions.[8−10] As well, chiral nanostructures can be a very interesting route for achieving negative refractive index phenomena.[11,12]

Chirality in NCs, as indicated by circular dichroism (CD) and UV−visible absorption spectra, is believed to originate from either chiral NC cores or adsorption patterns/surface distortion induced by chiral stabilizers.[13−22] The source of CD activity of NCs is still being debated and is most often associated with the, so-called, chiral surface defects, which are formed in response to the interaction of stabilizers and the crystal lattice

[†] National Centre for Nanoscience and Technology.
[‡] Department of Chemical Engineering, University of Michigan.
[§] Department of Materials Science and Engineering, University of Michigan.

(1) Alivisatos, A. P. *Science* **1996**, *271*, 933–937.
(2) Klimov, V. I.; Mikhailovsky, A. A.; Xu, S.; Malko, A.; Hollingsworth, J. A.; Leatherdale, C. A.; Eisler, H. J.; Bawendi, M. G. *Science* **2000**, *290*, 314–317.
(3) Bruchez, M., Jr.; Moronne, M.; Gin, P.; Weiss, S.; Alivisatos, A. P. *Science* **1998**, *281*, 2013–2016.
(4) Brus, L. *J. Phys. Chem.* **1986**, *90*, 2555–2560.
(5) Ekimov, A. I.; Efros, A. L.; Onushchenko, A. A. *Solid State Commun.* **1985**, *56*, 921–924.
(6) Moloney, M. P.; Gun'ko, Y. K.; Kelly, J. M. *Chem. Commun.* **2007**, *38*, 3900–3902.
(7) Elliott, S. D.; Moloney, M. P.; Gun'ko, Y. K. *Nano Lett.* **2008**, *8*, 2452–2457.
(8) Ahmadi, A.; Attard, G. *Langmuir* **1999**, *15*, 2420–2424.
(9) Hofstetter, O.; Hofstetter, H.; Wilchek, M.; Schurig, V.; Green, B. S. *Nat. Biotechnol.* **1999**, *17*, 371–374.
(10) Noguez, C.; Garzon, I. L. *Chem. Soc. Rev.* **2009**, *38*, 757–771.
(11) Pendry, J. B. *Science* **2004**, *306*, 1353–1355.
(12) Decker, M.; Klein, M. W.; Wegener, M.; Linden, S. *Opt. Lett.* **2007**, *32*, 856–858.
(13) Gautier, C.; Bürgi, T. *J. Am. Chem. Soc.* **2008**, *130*, 7077–7084.
(14) Kuhnle, A.; Linderoth, T. R.; Hammer, B.; Besenbacher, F. *Nature* **2002**, *415*, 891–893.
(15) You, C.-C.; Agasti, S. S.; Rotello, V. M. *Chem.—Eur. J.* **2008**, *14*, 143–150.
(16) Li, T.; Park, H. G.; Lee, A.-S.; Choi, A.-H. *Nanotechnology* **2004**, *10*, S660–S663.
(17) Bieri, M.; Gautier, C.; Bürgi, T. *Phys. Chem. Chem. Phys.* **2007**, *9*, 671–688.
(18) Schaaff, T. G.; Knight, G.; Shafigullin, M. N.; Borkman, R. F.; Whetten, R. L. *J. Phys. Chem. B* **1998**, *102*, 10643–10646.
(19) Schaaff, T. G.; Whetten, R. L. *J. Phys. Chem. B* **2000**, *104*, 2630–2641.
(20) Yao, H.; Miki, K.; Nishida, N.; Sasaki, A.; Kimura, K. *J. Am. Chem. Soc.* **2005**, *127*, 15536–15543.
(21) Nishida, N.; Yao, H.; Ueda, T.; Sasaki, A.; Kimura, K. *Chem. Mater.* **2007**, *19*, 2831–2841.
(22) Nakashima, T.; Kobayashi, Y.; Kawai, T. *J. Am. Chem. Soc.* **2009**, *131*, 10342–10343.

10.1021/ja906894r

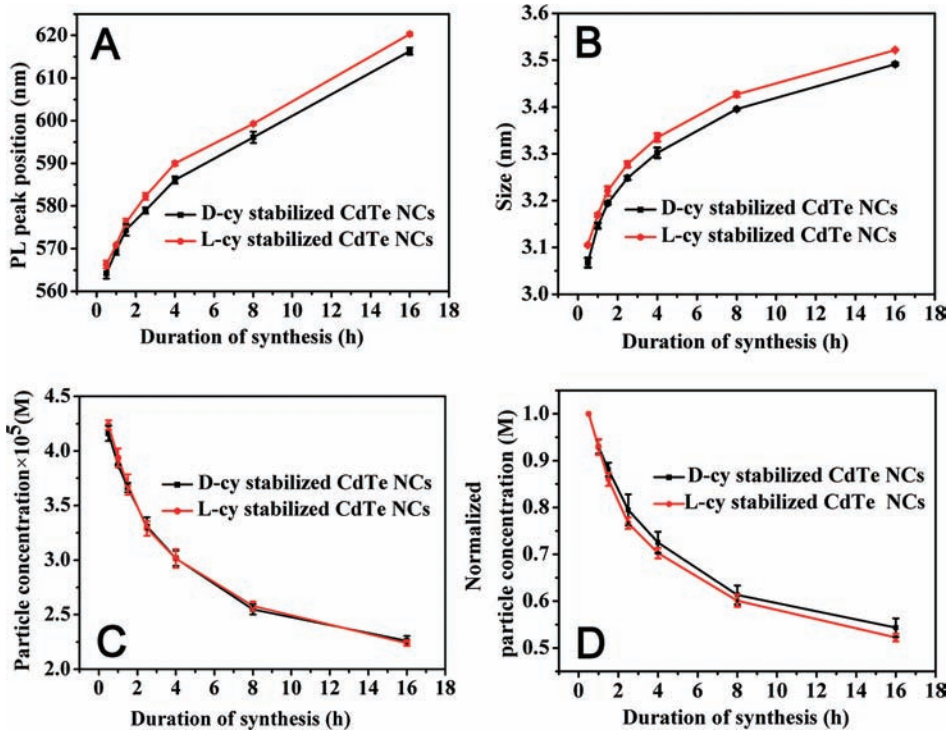

Figure 1. Temporal evolution of PL peak (A), particle size (B), particle concentration (C), and normalized particle concentration (D) of CdTe NCs stabilized by chiral cysteine. All data are average values obtained from at least five different experiments. Note the short error bars indicating the reproducibility of CdTe NC synthesis and statistical significance of the measurements (detailed data are listed in Table S1 in the Supporting Information).

of the NCs. Overall, the understanding of chiral properties of nanocolloids and the structures of these chiral surface defects is quite vague. Neither the atomic arrangements of the chiral defects nor the thermodynamic reasons behind the difference of the interactions of left- and right-rotating stabilizers with NCs have been put forward.

In this article, we seek to gain a deeper understanding of the structural origin of chirality in NCs. Among the different types of chiral molecules, the amino acid cysteine was selected as a stabilizer, because chiral bioorganic molecules, such as amino acids and polypeptides, are well known to play important roles in both biological functions and the evolution process of many biomaterials.[23,24] For example, chiroselective adsorption of amino acids onto mineral surfaces gives rise to the formation of chiral crystals with different structures.[25−28] The results obtained here indicate that chirality of the stabilizers leads not only to the appearance of CD peaks in NCs but also to a kinetic effect on their growth. The effect is small but very distinct and overall quite unexpected. This also sheds more light on the origin of stabilizer-induced chirality in nanoparticles, which is still uncertain. The potential structure of the chiral centers on the surface of NCs is proposed, and extensive microscopy and spectroscopic data are collected that confirm the idea of the topological similarity of chiral centers in inorganic nanoparticles and organic compounds. The difference in interactions of NCs with chiral stabilizers is likely to originate from tetrahedral atomic arrangements typical for II−VI semiconductors crystallizing in a cubic crystal lattice. Tetrahedral patterns have an intrinsic ability to generate chiral structures when all four atoms in the apexes are different. The actual molecular structure of chiral centers on CdTe surface is suggested and supported by quantum mechanical calculations. The thermodynamic characteristics of interactions between chiral centers and chiral stabilizers correlate very well with the experimental observations from NC growth kinetics and structural data obtained from the NCs.

Experimental Section

Synthesis of Water-Soluble (D,L)-Cysteine-Stabilized CdTe NCs. The general procedure of synthesis followed the Rogach−Weller method.[29] All chemicals used were of analytical grade or the highest purity available. Briefly, H_2Te gas (generated by the reaction of 0.05 g of Al_2Te_3 lumps with 4 mL of 0.5 M H_2SO_4 under an N_2 atmosphere) was passed through a nitrogen-saturated $Cd(ClO_4)_2 \cdot 6H_2O$ aqueous solution (0.013 M, 32 mL) at pH 11.2 in the presence of (D,L)-cysteine (178 mg) as a stabilizing agent. Then the reaction mixture was refluxed at 110 °C in an oil bath under N_2 gas for different periods of time. In order to avoid the possible effects of gas flow on the growth kinetics of the NCs, the flow rate of the N_2 gas was accurately controlled to 100 mL/min during the whole synthesis process.

Temporal Spectra Measurement. UV−vis absorption spectroscopy (Hitachi U-3010) and photoluminescence spectroscopy (Horiba Jobin Yvon FM-4) were conducted to record the temporal

(23) Xu, A.-W.; Ma, Y.; Colfen, H. *J. Mater. Chem.* **2007**, *17*, 415–449.
(24) Mann, S.; Archibald, D. D.; Didymus, J. M.; Douglas, T.; Heywood, B. R.; Meldrum, F. C.; Reeves, N. J. *Science* **1993**, *261*, 1286–1292.
(25) Maruyama, M.; Tsukamoto, K.; Sazaki, G.; Nishimura, Y.; Vekilov, P. G. *Cryst. Growth Des.* **2009**, *9*, 127–135.
(26) Orme, C. A.; Noy, A.; Wierzbicki, A.; McBride, M. T.; Grantham, M.; Teng, H. H.; Dove, P. M.; DeYoreo, J. J. *Nature* **2001**, *411*, 775–779.
(27) Wolf, S. E.; Loges, N.; Mathiasch, B.; Panthöfer, M.; Mey, I.; Janshoff, A.; Tremel, W. *Angew. Chem., Int. Ed.* **2007**, *46*, 5618–5623.
(28) Hazen, R. M.; Filley, T. R.; Goodfriend, G. A. *Proc. Natl. Acad. Sci. U. S. A.* **2001**, *98*, 5487–5490.
(29) Gaponik, N.; Talapin, D. V.; Rogach, A. L.; Hoppe, K.; Shevchenko, E. V.; Kornowski, A.; Eychmuller, A.; Weller, H. *J. Phys. Chem. B* **2002**, *106*, 7177–7185.

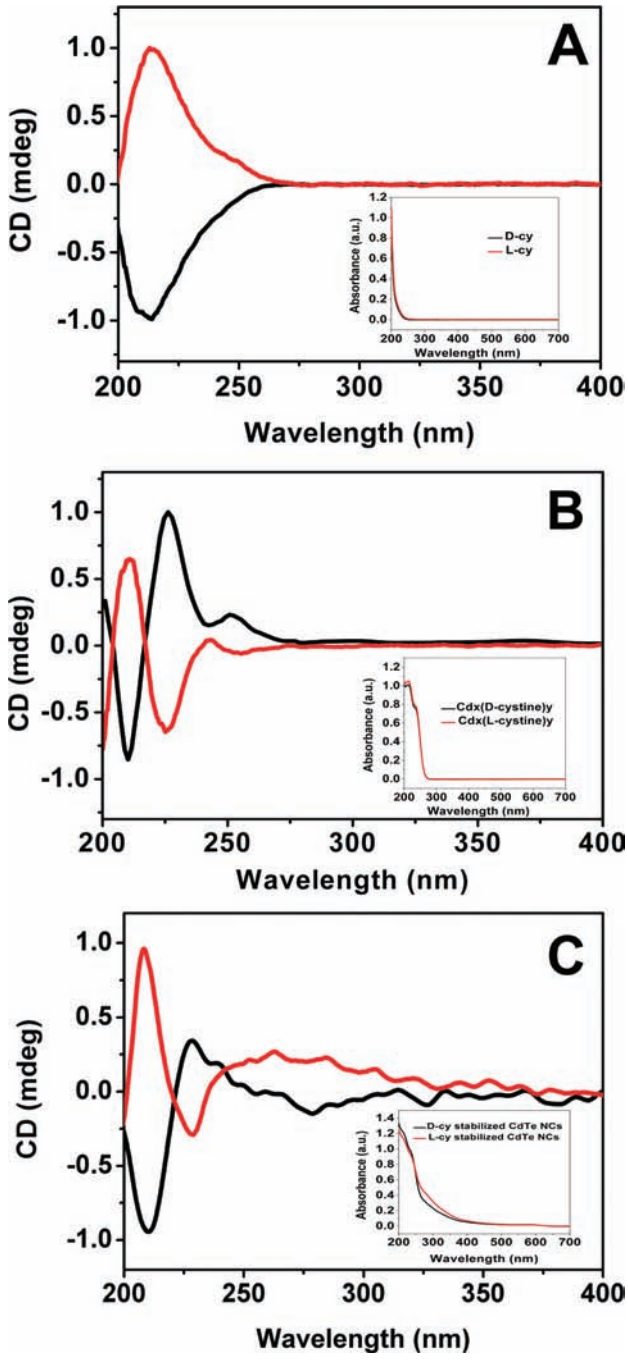

Figure 2. CD spectra of (A) L-cysteine (red) and D-cysteine (black); (B) complexes of L-cysteine and $Cd(ClO_4)_2 \cdot 6H_2O$ at pH 11.2 (red) and complexes of D-cysteine and $Cd(ClO_4)_2 \cdot 6H_2O$ at pH 11.2 (black); (C) L-cysteine-stabilized CdTe NCs (red) and D-cystine-stabilized CdTe NCs (black) after 16 h of synthesis. Insets present the corresponding UV−vis spectra.

optical properties of CdTe NCs stabilized by chiral cysteine at room temperature. The NC samples for spectral measurement were all diluted with phosphate buffer solution (pH 7.4) until their absorption at 480 nm was below 0.1. CD spectra were recorded by a Jasco J-810 spectropolarimeter in aqueous solution.

X-ray Photoelectron Spectroscopy (XPS) and Solid ^{13}C Nuclear Magnetic Resonance (NMR). A Kratos DLD Axis Ultra XPS using a monochromated Al source with an energy resolution of ~0.5 eV was applied to the surface of the NCs, and the power of the X-ray was 98 W (HT 14 kV and emission current 7 mA). High-resolution scans with a good signal ratio were obtained in the C 1s, N 1s, O 1s, S 2p, Cd 3d, and Te 3d regions of the spectrum. The quantitative analysis was based on the determination of the C 1s, N 1s, O 1s, S 2p, Cd 3d, and Te 3d peak areas with 0.278, 0.477, 0.780, 0.668, 6.623, and 9.508 as sensitivity factors, respectively. The chemical shift of ^{13}C of cysteine was conducted on a Bruker Advance III 400 spectrometer with a Doty Scientific Inc. 5 mm probe using silicon nitride rotors.

Purification of the (D,L)-Cysteine-Stabilized CdTe NCs. All the NC samples subjected to CD, XPS, NMR, IR, TEM, and XRD characterizations were centrifuged and precipitated as follows: 5 mL of 2-propanol was added into 5 mL of (D,L)-cysteine-stabilized CdTe NC crude solution, and the solution immediately became turbid. After centrifugation at 10 000 rpm for 5 min, the precipitates of the CdTe NPs were obtained. The precipitates were dried under vacuum and kept in the dark under the protection of argon gas until use.

Results and Discussion

The growth kinetics of CdTe NCs stabilized by chiral cysteine was investigated by recording the temporal dependence of their UV−visible absorption and the photoluminescence (PL) spectra (Figure 1 and Figure S1 in the Supporting Information). Using the well-established empirical equations,[30,31] we can calculate both the sizes and concentrations of CdTe NCs in solution from the PL and absorption spectra, respectively (Table S1 in the Supporting Information). Interestingly, measurements on both PL peak positions (Figure 1A) and the NC sizes (Figure 1B) show that the growth rate of CdTe NCs stabilized by D-cysteine (D-cy) *is slower* than those stabilized by L-cysteine (L-cy) (Figure S2 in the Supporting Information). Also, analysis of normalized concentrations of NC at varying reaction times to initiate the NCs after 30 min reaction time demonstrates that the concentration decrease of CdTe NCs stabilized by D-cysteine is slower than those stabilized by L-cysteine (Figure 1D). On the basis of these empirical observations, one can conclude that D-cysteine has a stronger interaction with CdTe cores compared with L-cysteine (Figure 1B,C). During the growth process dominated by Ostwald ripening, CdTe NCs with large sizes further grow at the expense of the small size NCs, and thus the sizes of the CdTe NCs gradually increase with a simultaneous decrease of their concentrations. Again, due to stronger interactions, D-cysteine-stabilized CdTe NCs are more stable, so both their size increase and concentration decrease are slower compared to L-cysteine-stabilized CdTe NCs. It should be stressed that the chirality difference in the growth kinetics of NCs can hardly be explained by the classical growth theory of NCs, which focuses on the effect of grafting density and adhesion energy of organic stabilizers on *achiral* inorganic cores.[32,33]

The chiral properties of CdTe NCs stabilized by different enantiomers of cysteine were characterized by their absorption spectra (Figure 2). Although all the UV−vis spectra are identical (insets in Figure 2), opposite peaks in the CD spectra are observed for cysteine enantiomers (Figure 2). With respect to pure cysteine, the additional chiral features appear at 225 and 250 nm for the mixture of Cd cations and chiral cysteine (Figure 2B), which can be ascribed to formation of a Cd_x(cystine)$_y$

(30) Yu, W. W.; Qu, L.; Guo, W.; Peng, X. *Chem. Mater.* **2003**, *15*, 2854–2860.
(31) Rogach, A. L.; Franzl, T.; Klar, T. A.; Feldmann, J.; Gaponik, N.; Lesnyak, V.; Shavel, A.; Eychmuller, A.; Rakovich, Y. P.; Donegan, J. F. *J. Phys. Chem. C* **2007**, *111*, 14628–14637.
(32) Schmid, G., Ed. *Nanoparticles: From Theory to Application*; John Wiley & Sons: Weinheim, Germany, 2004.
(33) Yin, Y.; Alivisatos, A. P. *Nature* **2005**, *437*, 664–670.

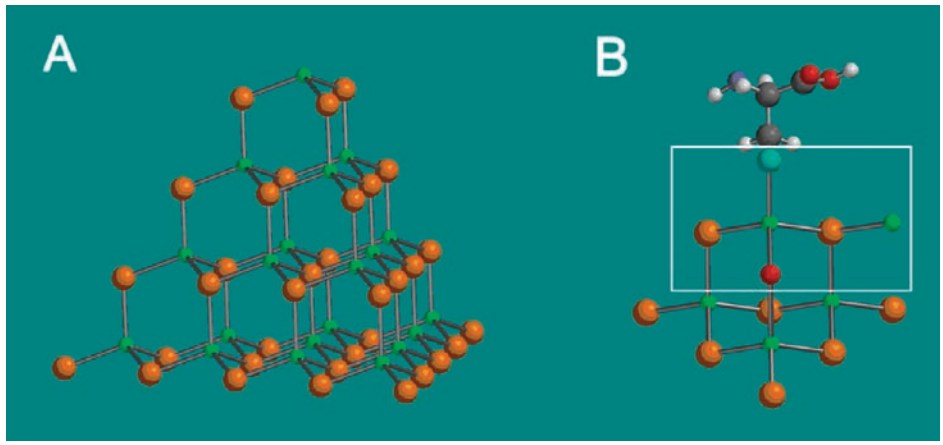

Figure 3. (A) Ideal tetrahedron of CdTe NCs used in calculations and (B) model of the chiral tetrahedral apex: Cd (green); Te (brown); O (red); S (cyan).

Table 1. Surface Atom Percentage of (D,L)-Cysteine-Stabilized CdTe NCs

	Cd						
	Cd-Te	Cd-O	Te	C[a]	O[a]	N	S
D-cysteine-stabilized CdTe NCs	5.6	2.1	5.6	55.5	26.7	2.3	2.3
L-cysteine-stabilized CdTe NCs	4.9	1.4	4.8	58.8	26.3	1.8	2.0

[a] Due to the possible exposure of the NC surface to C and O, the amount of C and O is higher than the stoichiometric ratio of cysteine molecules.

complex.[34] Compared with cysteine (Figure 2A) and the mixture of (D,L)-cysteine and $Cd(ClO_4)_2 \cdot 6H_2O$ at pH 11.2 (Figure 2B), which present prominent peaks at 210, 225 and 250 nm, CdTe NCs stabilized by chiral cysteine show additional broad CD features between 250 and 350 nm. Thus, cysteine molecules adsorbed on NC surfaces not only preserve their own chirality but also induce chirality on the CdTe core. Considering the trapped states, they are typically characterized by a wide range of energies. Therefore the width of the corresponding CD bands will be wider than those for the valence band−conductive band transitions. Indeed, the diffuse shape in the CD signal can be attributed to a spectrum of the chiral units on the NC cores, especially in the range 250−350 nm, where NCs have strong absorption features (inset in Figure 2C).[22]

Now the questions arise, how do cysteine molecules induce changes in the CdTe surface to generate the chiral response, and why do the D-cysteine molecules have a stronger interaction with the CdTe cores compared to L-cysteine? In order to understand the effect of the stabilizers' chirality on the structures and optical properties of semiconductor NCs, quantum mechanical calculations of the energy of cysteine binding to CdTe NC surfaces are carried out. Considering that the chiral structure induced by chiral ligands is on the surface of NCs, a typical tetrahedral CdTe NC with 20 Cd atoms and 34 Te atoms is used as the basis for calculations, and the size of the model compound is about 1.7 nm (Figure 3A). It is structurally analogous to the tetrahedral cluster that we used for analyzing CdS NCs previously.[35] For simplicity, the atomic model assumes that only one apex of the CdTe tetrahedron has an exposed Cd atom available for attachment of cysteine. Considering the strong interaction between thiol and the Cd atom, cysteine is attached to the CdTe tetrahedron by building a Cd−S bond to the exposed Cd atom (Figure 3B).

Very recently, the origin of chirality of penicillamine-stabilized CdS NCs was explained by DFT calculations, and the ligands were found packing into helical bands on the surface, which distorted the outermost Cd atoms and thus transmitted the enantiomeric structure to the surface layers.[7] However, it is difficult to expect the same degree of packing and surface distortion in the underlying semiconductor from a small molecule, such as cysteine. Hence, we need to consider the chirality from a different point of view, which is probably more straightforward and universal. It is well known in organic chemistry that a carbon atom with four different substituents forms a chiral center. A similar situation can potentially exist in NCs, as well. In zinc-blende CdTe (Figure S3 in the Supporting Information), Cd and Te atoms are four-coordinated, forming tetrahedrons.[36] In an ideal case, all four Te atoms are identical and surround Cd at the perfect tetrahedral angle. If all four atoms in this tetrahedron are different in some way, a chiral center is formed. These atoms may actually be of the same element, say, Te atoms, as long as they are not symmetrically related and do have different atomic groups attached to them. This structure can also be compared to chiral centers in organic chemistry when four carbon atoms belonging to four different ligands around a basic methane tetrahedron produce a CD-active molecule.

Let us focus, for instance, on one tetrahedral apex of one tetrahedral semiconductor NC that consists of Cd, a chiral cysteine ligand, and three Te atoms (Figure 3A). All three of these atoms need to be chemically different from each other for this apex to display chirality. Due to the high reactivity of the NC surface, the coordination of the exposed Cd atoms can be significantly different compared to those inside the NC core. The presence of OH^- in the synthetic solution favors formation of a Cd−O bond on the surface of the CdTe NCs, and accordingly, one of the Te atoms in the apex tetrahedron can be replaced by one O atom. This modification is quite reasonable considering the actual conditions of NC synthesis taking place in a highly basic media of pH 11.2. Also from a chemical point of view, the bond energy of Cd−O (236 ± 84 kJ/mol) is larger than those of Cd−Te (100 ± 15.1 kJ/mol) and Cd−S (208.5 ± 20.9 kJ/mol),[37] and oxygen, sulfur, and tellurium belong to the same main group and the model of covalent bond is similar.

(34) Jalilehvand, F. *Chem. Soc. Rev.* **2006**, *35*, 1256–1268.
(35) Shanbhag, S.; Kotov, N. A. *J. Phys. Chem. B* **2006**, *110*, 12211–12217.
(36) Tang, Z.; Kotov, N. A.; Giersig, M. *Science* **2002**, *297*, 237–240.
(37) Lide, D. R., Ed. *CRC Handbook of Chemistry and Physics, Internet Version*, 87th ed.; Taylor and Francis Group: Boca Raton, FL, 2007; pp 9−56.

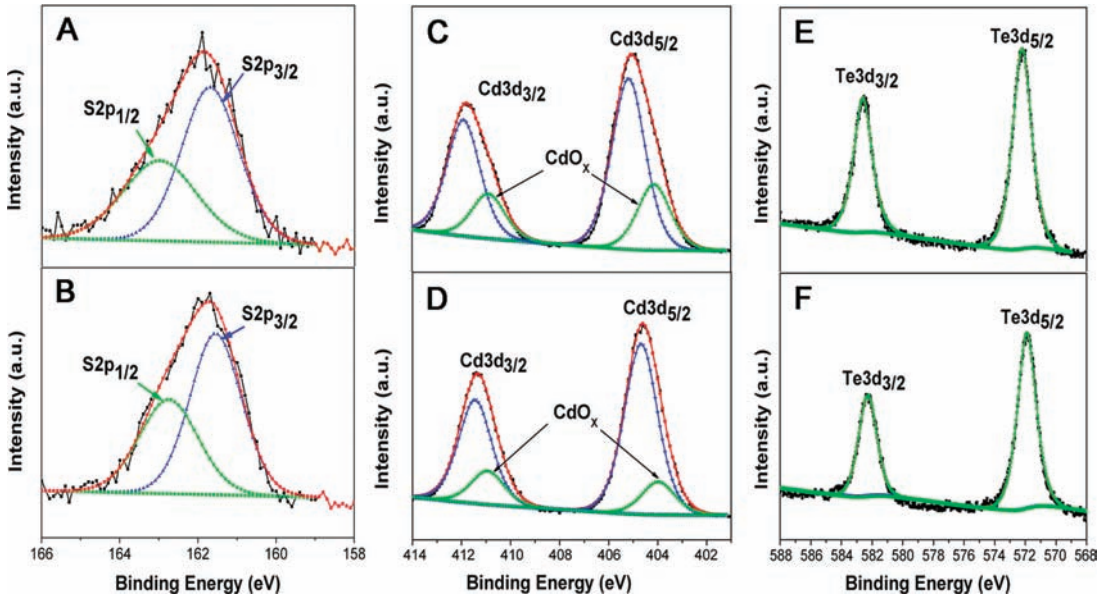

Figure 4. X-ray photoelectron spectra of D-cysteine-stabilized CdTe NCs (A, C, E) and L-cysteine-stabilized CdTe NCs (B, D, F). The spectra are fitted with Pseudo−Voigt (GL) functions with a combined polynomial and Shirley background.

Table 2. Chemical Shifts (ppm) of the ^{13}C Solid-State NMR Shown in Figure S6

	$^{13}\underline{C}$-S	$^{13}\underline{C}$-N		$^{13}\underline{C}$OO	
D-cysteine	26.5	55.8		170.3	
L-cysteine	26.5	55.8		170.3	
D-cysteine-stabilized CdTe NCs	33.9	59.0	55.1	179.9	175.0
L-cysteine-stabilized CdTe NCs	33.9	59.0	55.1	179.9	175.0

The importance of Cd−O for formation of chiral NCs is confirmed by altering the ratio of Cd−O bonds on NC surfaces (Figure S4 in the Supporting Information). Then, another Te atom in the apex can be attached to one additional Cd ion. It is also highly plausible because during the growth of CdTe NCs new atoms of Cd must form new bonds to the atoms of Te. In this situation, all four substituents around the central atom of the tetrahedron, i.e., the Cd atoms, become chemically different, and the entire center becomes chiral (white square in Figure 3B). From the XPS results (Table 1), one can see that the amount of Cd is more than the stoichiometric amount with respect to Te, which coincides with the idea that some extra Cd ions/atoms compared to Te atoms serve as apexes of the tetrahedron. A similar nonstoichiometric Cd/Te ratio for NCs is also observed in the previous report.[38] Moreover, the presence of Cd−O bonds on the surface of NCs also supports the idea of Te replacement with O atoms, as depicted in Figure 3.

One should consider this as an example of how the chiral centers can form based on the prototypical tetrahedral structure around Cd. There is a large variety of potential chemically different "substituents" around both Cd and Te centers. However, in this study we shall use one general type of model structure to explain the observed experimental data. One certainly needs to realize that the suggested structure of the chiral center (Figure 3B) can be somewhat different and even change from NC to NC. As shown in Table 1, the atom percentages of (D,L)-cysteine stabilizers on CdTe NC surfaces have slight differences, and this implies different environments on the NC surfaces.

The surface state of cysteine-stabilized CdTe NCs can be revealed by a detailed analysis of the binding energies from XPS spectra (Figure 4 and Figure S5 in the Supporting Information). The S 2p spectral regions (Figure 4A,B) show two symmetric peaks representative of the 2p3/2 and 2p1/2 splitting induced by the spin−orbit interaction. We do not see any obvious difference in the binding energy between D-cysteine-stabilized CdTe NCs and L-cysteine-stabilized CdTe NCs. As expected, the binding energies at 161.5 eV (S 2p3/2) and 162.7 eV (S 2p1/2) indicate formation of a Cd−S bond between cysteine and the surface of NCs.[39,40] In the Cd 3d core level regions (Figure 4C,D), the signals are characterized by an asymmetric peak on the low binding energy side (green dotted curves), which can be assigned to a Cd−O bond.[41,42] Importantly, the XPS results are consistent with the hypothesis outlined above and the general type of model structures where O atoms have a covalent bond with a surface Cd atom. The Te 3d spectral signals show two symmetric peaks representative of the 3d3/2 and 3d5/2 splitting induced by the spin−orbit interaction. Again, there is no obvious difference in the binding energy between D-cysteine-stabilized CdTe NCs and L-cysteine-stabilized CdTe NCs.

Some information about the conformation of the cysteine stabilizers on NC surfaces can also be obtained from the NMR results. As shown in Table 2, a stronger coordination between cysteine stabilizers and CdTe core through S−Cd bonds is confirmed on the basis of the obvious shift to low field for the chemical shift of $^{13}\underline{C}$-S. Notably, there are no free molecules of cysteine because there is no splitting in the C-S carbon atom that is located in the immediate vicinity of the NC surface. On the contrary, splitting of the $^{13}\underline{C}$-N and $^{13}\underline{C}$OO signals shows

(38) Rockenberger, J.; Troger, L.; Rogach, A. L.; Tischer, M.; Grundmann, M.; Eychmuller, A.; Weller, H. *J. Chem. Phys.* **1998**, *108*, 7807–7815.
(39) Cavalleri, O.; Gonella, G.; Terreni, S.; Vignolo, M.; Floreano, L.; Morgante, A.; Canepa, M.; Rolandi, R. *Phys. Chem. Chem. Phys.* **2004**, *6*, 4042–4046.
(40) Borchert, H.; Talapin, D. V.; Gaponik, N.; McGinley, C.; Adam, S.; Lobo, A.; Moller, T.; Weller, H. *J. Phys. Chem. B* **2003**, *107*, 9662–9668.
(41) Katari, J. E. B.; Colvin, V. L.; Alivisatos, A. P. *J. Phys. Chem.* **1994**, *98*, 4109–4117.
(42) Lobo, A.; Borchert, H.; Talapin, D. V.; Weller, H.; Möler, T. *Colloids Surf., A* **2006**, *286*, 1–7.

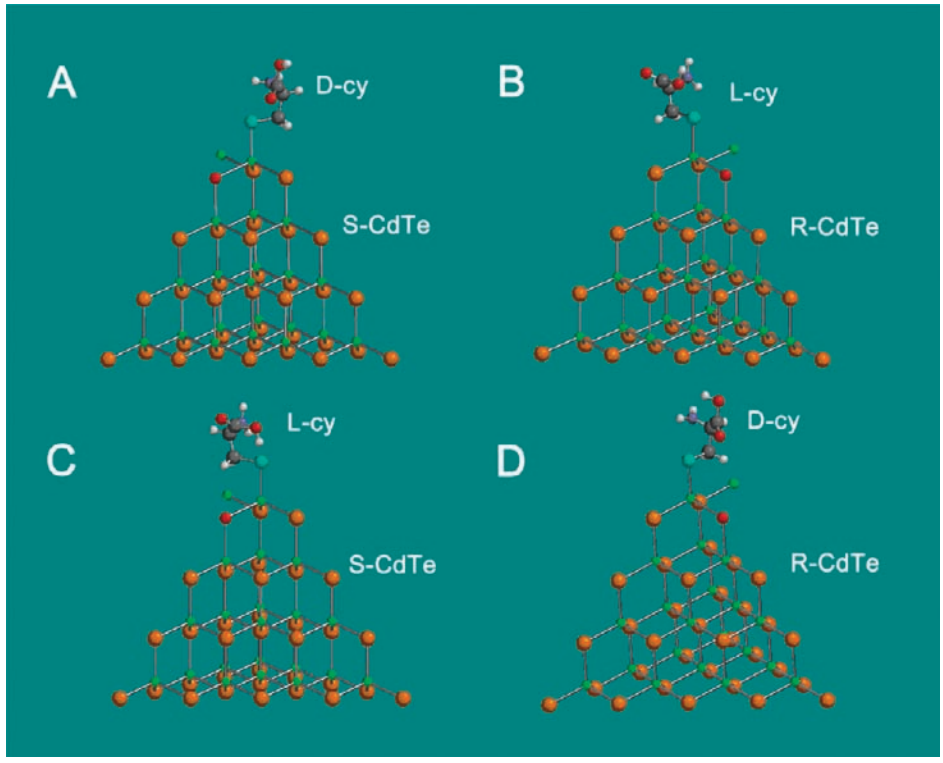

Figure 5. Model of four different chiral pairs of cysteine and CdTe: (A) (D-cy, *S*-CdTe), (B) (L-cy, *R*-CdTe), (C) (L-cy, *S*-CdTe), and (D) (D-cy, *R*-CdTe). Atoms: Cd (green); Te (brown); O (red); H (light); S (cyan); C (gray).

Table 3. Calculation Results Based on the CdTe Atomic Model

	D-cy	L-cy
S-CdTe	9242.0 ± (0.169) kcal/mol	9259.2 ± (0.001) kcal/mol
R-CdTe	9255.9 ± (0.007) kcal/mol	9242.0 ± (0.003) kcal/mol

that both the amino and carboxylic acid groups of cysteine molecules on the surface of CdTe exist at least in two different environments (Table 2 and Figure S6 in the Supporting Information). One of these conformations corresponds to the position with a greater degree of freedom for the movement of the carbon atoms in the C-N and COO groups and with ^{13}C NMR peaks located almost in the same places as for free cysteine (Table 2, chemical shifts at 55.1 ppm for $^{13}\underline{C}$-N and 175.0 ppm for $^{13}\underline{C}$OO). The other is likely to result from the partial intermolecular hydrogen bond between the carboxyl group and the amino group of cysteine stabilizers on the NC surfaces, leading to a downshift in their NMR spectra (Table 2, chemical shifts at 59.0 ppm for $^{13}\underline{C}$-N and 179.9 ppm for $^{13}\underline{C}$OO). Such results can be easily attributed to the apex cysteine molecules and similar structures in other places on the NC surface. Therefore, we can conclude that both XPS and NMR data are in agreement with the model presented in Figure 3B. A similar conclusion can be also drawn from IR spectral analysis (Figure S7 in the Supporting Information).

By simply changing the relative position of the O atom and additionally attached Cd atom, the CdTe enantiomers can be built. On the basis of the Cahn−Ingold−Prelog priority rules, one can denote the CdTe structures in Figure 5A,C as *S*, and the structures in Figure 5B,D as *R*. Correspondingly, there are four different chiral pairs of cysteine and CdTe: (D-cy, *S*-CdTe), (D-cy, *R*-CdTe), (L-cy, *R*-CdTe), and (L-cy, *S*-CdTe) (Figure 5). Note that once the two optical centers are combined, the pairs of opposite enantiomers may or may not be the mirror images of each other due to rotation around the connecting C−S bond. For instance, (D-cy, *S*-CdTe) (Figure 5A) and (L-cy, *R*-CdTe) (Figure 5B) may or may not be the mirror reflections of each other due to the additional degree of freedom and may, in fact, have (slightly) different thermodynamics due to differences in preferential arrangements of the atoms in space.

To clarify this property of the bichiral centers, the software package Spartan 04 (Wavefunction Inc., Irvine, CA) was used to calculate the energy difference in cysteine-CdTe enantiomers. The net formal charge on the built model is calculated from the atomic stoichiometry by associating Cd, Te, and O in the framework of CdTe NC with a charge of +2, −2, and −2, respectively, and the charge on cysteine is calculated to be −1 due to the absence of an H atom in the SH group. Correspondingly, the atomic model had a molecular structure of $[Cd_{21}Te_{33}O(C_3O_2NSH_6)]^-$.[27] The geometry of the NC models was first optimized by using the Merck molecular force field (MMFF) to allow the cysteine molecule, additional Cd, and substituted O atoms to relax. The optimization algorithm varied the bond lengths and angles (including rotation around the Cd−S bond) to find the lowest energy structures of CdTe NCs. For the thus-defined equilibrium geometry, the single-point energy mode was used to compute the energy of the atomic structure of a NC by the well-established semiempirical parameter model 3 algorithm (PM3). The energies reported below represent the sum of electronic, vibrational, rotational, nuclear, and translational energy components for a specific atomic model. The calculation results are summarized in Table 3. Note that for (D-cy, *S*-CdTe) and (L-cy, *R*-CdTe) pairs, the energies are nearly the same, while in the case of (L-cy, *S*-CdTe) and (D-cy, *R*-CdTe) pairs, the energies are quite different. The energy of the (D-cy, *R*-CdTe) pair is about 3.3 kcal/mol lower than that of the (L-cy, *S*-CdTe) pair. Note that in a thermodynamic sense this difference in energies is not that small. As a verification point,

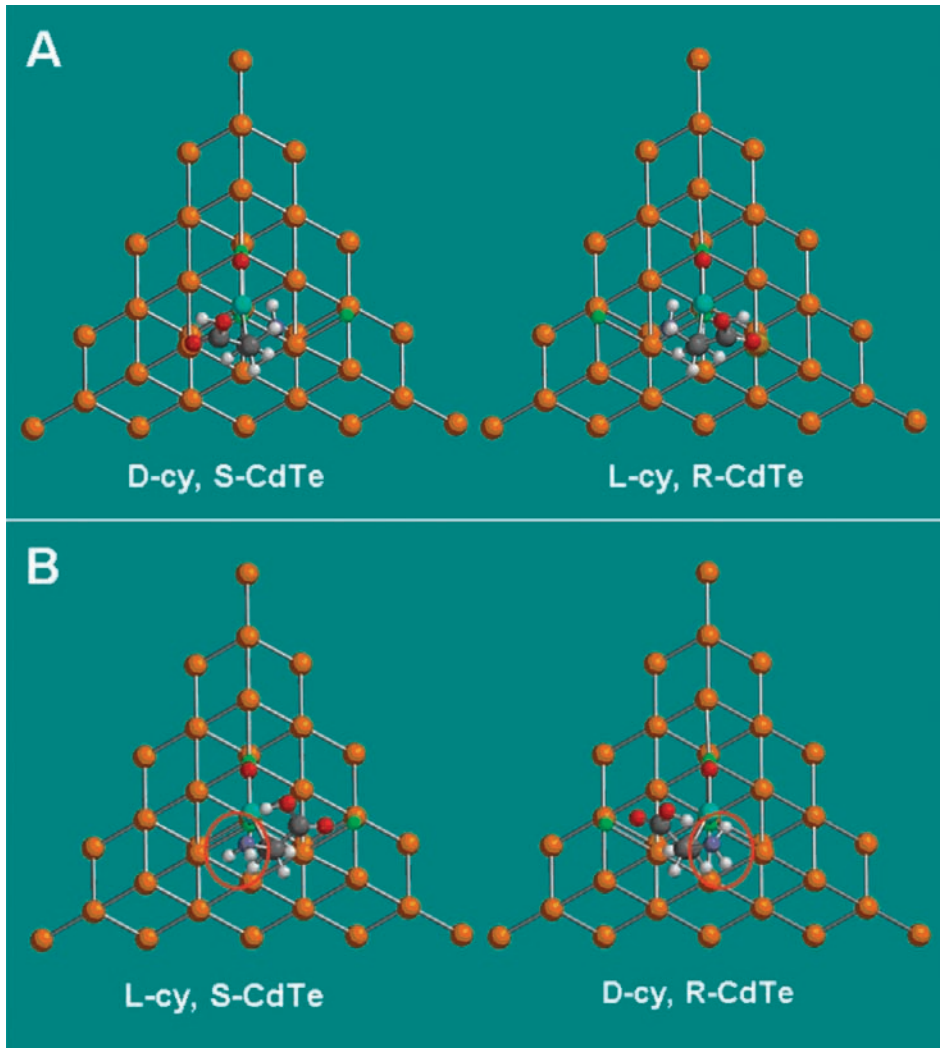

Figure 6. (A) Lowest energy configurations of (D-cy, *S*-CdTe) and (L-cy, *R*-CdTe) are nearly mirror images, and correspondingly, they have nearly the same energies. (B) Lowest energy configurations of (L-cy, *S*-CdTe) and (D-cy, *R*-CdTe) are not mirror images. The red ovals highlight the areas where the structural differences are particularly significant. Consequently, the energies of the two structures are different. Atoms: Cd (green); Te (brown); O (red); H (light); S (cyan); C (gray).

a similar energy difference was observed for adsorption of D- and L-cysteine on the Au (17 11 9) surface,[43] which validates the presented calculations. Also note that the energy difference of 3.3 kcal/mol is not that small and is comparable to the free energy of formation of gaseous ammonia ($\Delta_f G^0 = -3.921$ kcal/mol).[44] Moreover, one NC may have several chiral centers, for instance in four apexes of a tetrahedron, which may further exacerbate the effect of the arrangement of atoms in the bichiral centers on the yield of specific isomers.

Considering that the energies of (D-cy, *S*-CdTe) and (L-cy, *R*-CdTe) are the same, but the energy of (D-cy, *R*-CdTe) is lower than (L-cy, *S*-CdTe), NCs stabilized with D-cysteine should be on average more stable and, consequently, grow slower because the growth at this stage occurs primarily via Ostwald ripening and involves the detachment of a monomer from an existing NC. This correlates very well with our experimental results (Figure 1B,D). Furthermore, the energy of the (D-cy, *S*-CdTe) pair is noticeably lower than that of (D-cy, *R*-CdTe), which suggests that the preferred configuration of CdTe NCs is the *S* type when D-cysteine is used as a stabilizer. Analogous analysis also indicates that the preferred configuration is *R*-CdTe when the stabilizers are L-cysteine. This is also perfectly consistent with the observed CD spectra and explains quite well why CdTe NCs stabilized with cysteine with different chirality present opposite peaks in the 250−350 nm part of the CD spectrum (Figure 2C).

It might also be useful to point out that the similarity of energies between (D-cy, *S*-CdTe) and (L-cy, *R*-CdTe) implies they are the mirror images of each other in the relaxed state and, hence, have the same energy in achiral media.[45] In the case of (D-cy, *R*-CdTe) and (L-cy, *S*-CdTe) pairs, the minimum energy states have a considerable energy difference and are not mirror reflections of each other. This discrepancy is confirmed

(43) Greber, T.; ljivančanin, Ž. Š.; Schillinger, R.; Wider, J.; Hammer, B. *Phys. Rev. Lett.* **2006**, *96*, 056103(1−4) .

(44) Lide, D. R., Ed. *CRC Handbook of Chemistry and Physics, Internet Version*, 87th ed.; Taylor and Francis Group: Boca Raton, FL, 2007; pp 5−62.

(45) The calculations were carried out for vacuum conditions. In the first approximation the effect of the solvent, i.e., water, may be neglected because water is not a chiral medium as well. In a more general case, one should remember that the minimum energy state in one medium can be different from that in another, and hence, the conformations of the bichiral centers could be quite different.

Table 4. Calculation Results Based on the CdSe Atomic Model

	D-cy	L-cy
S-CdSe	10006.0 ± (0.645) kcal/mol	10027.0 ± (0.001) kcal/mol
R-CdSe	10024.0 ± (0.337) kcal/mol	10010.2 ± (0.023) kcal/mol

Table 5. Calculation Results Based on the CdTe Atomic Model When Penicillamine (pen) Is Used As a Stabilizer

	D-pen	L-pen
S-CdTe	9239.0 ± (0.034) kcal/mol	9275.0 ± (0.232) kcal/mol
R-CdTe	9259.2 ± (0.002) kcal/mol	9232.9 ± (0.003) kcal/mol

by the configurations of chiral cysteine on the surface of CdTe NCs at the minimum energy state (Figure 6). Overall, one can say that the rotational movement around the Cd−S bond in the bichiral center in the NCs holds the key to the thermodynamic differentiation and the greater amount of a specific enantiomer forming.

It might also be interesting to demonstrate how general the proposed chirality model of NCs based on the hypothesis of tetrahedral atomic arrangements with four different "susbstituents" really is. To this end, we carried out a similar theoretical study for cysteine-stabilized CdSe NCs and penicillamine-stabilized CdTe NCs to compare with the existing literature data.

After replacing all Te atoms with Se atoms in the atomic models and performing the appropriate geometry relaxation step, we can obtain the results shown in Table 4. The average energy of the (D-cy, *S*-CdSe) and (D-cy, *R*-CdSe) pairs is 10015.0 kcal/mol, and the average energy of the (L-cy, *S*-CdSe) and (L-cy, *R*-CdSe) pairs is 10018.6 kcal/mol, respectively. As one can see, the difference in average energy is significant and amounts to 3.6 kcal/mol. So, in accord with CdTe NPs, D-cysteine-stabilized CdSe NCs are more stable compared with L-cysteine-stabilized NCs. The difference between the NC isomers for one enantiomer of the stabilizer, when say only the D- or only the L-isomer of cysteine is used, can be as high as 10024.0−10006.0 = 18 kcal/mol. So, CdSe NCs will prefer the *R* type when L-cysteine is used and the *S* type when D-cysteine is used.

A change in stabilizers also leads to similar results. As shown in Table 5, the average energy of the (D-pen, *S*-CdTe) and (D-pen, *R*-CdTe) pairs is 9249.1 kcal/mol and the average energy of the (L-pen, *S*-CdTe) and (L-pen, *R*-CdTe) pairs is 9254.0 kcal/mol, respectively. The difference in average energy is about 4.9 kcal/mol. This result is also similar to that of cysteine-stabilized CdTe NCs. D-Penicillamine-stabilized CdTe NCs are more stable. CdTe NCs will prefer the *S* type when D-penicillamine is used and the *R* type when L-penicillamine is used. This chirality selection is also consistent with a previous report on CdS NCs capped with penicillamine enantiomers.[7]

Among other points made above, the data presented here indicate that one can potentially synthesize chiral NCs from a racemic mixture of the stabilizer due to the noticeable difference in thermodynamic parameters of the isomers. For instance, the D-form of cysteine seems to be preferentially bound to CdTe (Table 3) if the structure of the apexes is identical to that in Figure 3. For other chiral arrangements of the atoms in the apexes, the preference between L- and D-forms of the stabilizer might be different. This would be certainly quite fundamentally interesting although might not be as easy to observe as it seems because of a fairly large potential variety of chiral atomic tetrahedral arrangements in the apexes involving different atoms. Some of them will be favorable to right-rotating isomers and some to the left-rotating ones. Judicious control of synthetic conditions and further advances in the theoretical understanding of how two or more organic and NC chiroptical components can interact will certainly facilitate further advances in this direction.

Conclusions

In summary, we investigated the effect of the chiral amino acid cysteine on the optical properties of CdTe NCs. Combining both experimental observations and theoretical calculations, we elucidated the difference of both growth rate and product structure in CdTe NCs stabilized by cysteine with different chirality. The well-known concept of chirality in tetrahedral molecules with four different substituents known from organic chemistry is applied to understand the origin of chirality in NCs. This work opens the venue for understanding the chiral effects in nanoscale[46] and synthetic routes for the preparation of chiral inorganic nanocolloids.

Acknowledgment. The authors thank the 100-Talent Program of the Chinese Academy of Sciences (Z.Y.T.), the National Research Fund for Fundamental Key Project No. 2009CB930401 (Z.Y.T.), National High-tech Research and Development Program No. 2007AA03Z302 (Z.Y.T.), NSFC No. 20973047 (Z.Y.T.), NSF (N.A.K.), AFOSR (N.A.K.), and DARPA (N.A.K.) for the financial support of this research. We are also grateful to Prof. Weiping Zhang for help with NMR and useful discussions.

Supporting Information Available: Additional experimental details including UV−vis and photoluminescence, statistic optical spectral data, and XRD, TEM, XPS, NMR, and IR spectra further support the experimental and theoretical results. This information is available free of charge via the Internet at http://pubs.acs.org.

JA906894R

(46) Gautier, C.; Bürgi, T. In *Chirality at the Nanoscale: Nanoparticles, Surfaces, Materials and More*; Amabilino, D. B., Ed.; John Wiley and Sons: Weinheim, 2009; pp 67−91.